

Effective Electrostatic Interactions in Suspensions of Polyelectrolyte Brush-Coated Colloids

H. Wang* and A. R. Denton†

Department of Physics, North Dakota State University, Fargo, ND, 58105-5566

(Dated: July 15, 2018)

Abstract

Effective electrostatic interactions between colloidal particles, coated with polyelectrolyte brushes and suspended in an electrolyte solvent, are described via linear response theory. The inner cores of the macroions are modeled as hard spheres, the outer brushes as spherical shells of continuously distributed charge, the microions (counterions and salt ions) as point charges, and the solvent as a dielectric continuum. The multi-component mixture of macroions and microions is formally mapped onto an equivalent one-component suspension by integrating out from the partition function the microion degrees of freedom. Applying second-order perturbation theory and a random phase approximation, analytical expressions are derived for the effective pair interaction and a one-body volume energy, which is a natural by-product of the one-component reduction. The combination of an inner core and an outer shell, respectively impenetrable and penetrable to microions, allows the interactions between macroions to be tuned by varying the core diameter and brush thickness. In the limiting cases of vanishing core diameter and vanishing shell thickness, the interactions reduce to those derived previously for star polyelectrolytes and charged colloids, respectively.

PACS numbers: 82.70.Dd, 82.45.-h, 05.20.Jj

*Electronic address: hao.wang@ndsu.nodak.edu

†Electronic address: alan.denton@ndsu.nodak.edu

I. INTRODUCTION

Polyelectrolytes [1, 2] are ionizable polymers that dissolve in a polar solvent, such as water, through dissociation of counterions. Solutions of polyelectrolytes are complex mixtures of macroions and microions (counterions and salt ions) in which direct electrostatic interactions between macroions are screened by surrounding microions. Polyelectrolyte chains, grafted or adsorbed by one end to a surface at high concentration, form a dense brush that can significantly modify interactions between surfaces in solution. When attached to colloidal particles, *e.g.*, latex particles in paints or casein micelles in milk [3], polyelectrolyte brushes can stabilize colloidal suspensions by inhibiting flocculation [4, 5]. Biological polyelectrolytes (biopolymers), such as proteins in cell membranes, can modify intercellular and cell-surface interactions.

Conformations and density profiles of polyelectrolyte (PE) brushes have been studied by a variety of experimental, theoretical, and simulation methods, including dynamic light scattering [6], small-angle neutron scattering [7, 8, 9], transmission electron microscopy [9], neutron reflectometry [10], surface adsorption [11], atomic force microscopy [12], self-consistent field theory [13, 14, 15, 16, 17, 18, 19], scaling theory [18, 19, 20, 21], Poisson-Boltzmann theory [22], Monte Carlo simulation [22], and molecular dynamics simulation [23, 24]. Comparatively few studies have focused on electrostatic interactions between PE brush-coated surfaces. Interactions between neutral surfaces – both planar and curved (spherical) – with grafted PE brushes have been modeled using scaling theory [20], while interactions between charged surfaces coated with oppositely-charged PEs have been investigated for planar [22] and spherical (colloidal) surfaces [25] via Monte Carlo simulation and a variety of theoretical methods.

While microscopic models that include chain and microion degrees of freedom provide the most realistic description of PE brushes, simulation of such explicit models for more than one or two brushes can be computationally demanding. The purpose of the present paper is to develop an alternative, coarse-grained theoretical approach, based on the concept of effective interactions, which may prove useful for predicting thermodynamic and other bulk properties of suspensions of PE brush-coated colloids. Modeling each brush as a spherical shell of continuously distributed charge, we adapt linear response theory, previously developed for

charged colloids [26, 27, 28] and PEs [29], to derive effective electrostatic interactions. The theory is based on mapping the multi-component mixture onto an equivalent one-component system of “pseudo-macroions” by integrating out from the partition function the degrees of freedom of the microions. Within the theory, microions play three physically important roles: reducing (renormalizing) the bare charge on a macroion; screening direct Coulomb interactions between macroions; and generating a one-body volume energy. The volume energy – a natural by-product of the one-component reduction – contributes to the total free energy and can significantly influence thermodynamic behavior of deionized suspensions.

Outlining the remainder of the paper, Sec. II defines the model suspension of PE brush-coated colloids; Sec. III reviews the linear response theory; Secs. IV and V present analytical and numerical results for counterion density profiles, effective pair interactions, and volume energies in bulk suspensions; and finally, Sec. VI summarizes and concludes.

II. MODEL

The system of interest is modeled as a suspension of N_m spherical, core-shell macroions of charge $-Ze$ (valence Z), core radius a , and PE brush shell thickness l (outer radius $R = a + l$), and N_c point counterions of charge ze in an electrolyte solvent in volume V at temperature T (see Fig. 1). The core is assumed to be neutral, the macroion charge coming entirely from the PE shell. Assuming a symmetric electrolyte and equal salt and counterion valences, the electrolyte contains N_s point salt ions of charge ze and N_s of charge $-ze$. The microions thus number $N_+ = N_c + N_s$ positive and $N_- = N_s$ negative, for a total of $N_\mu = N_c + 2N_s$. Global charge neutrality in a bulk suspension constrains macroion and counterion numbers via $ZN_m = zN_c$. Number densities of macroions, counterions, and salt ions are denoted by n_m , n_c , and n_s , respectively. Within the primitive model of ionic liquids [30], the solvent is treated as a dielectric continuum of dielectric constant ϵ , which acts only to reduce the strength of Coulomb interactions between ions.

In PE solutions, the counterions can be classified into four regions: (1) those within narrow tubes enclosing the PE chains, of radius comparable to the Bjerrum length, $\lambda_B = e^2/(\epsilon k_B T)$; (2) those outside of the tubes but still closely associated with the chains; (3) those not closely associated with the chains, but still inside of the PE shells; and (4) those entirely

outside of the macroions. Counterions in regions (1)-(3) can be regarded as trapped by the macroions, while those in region (4) are free to move throughout the suspension. Within region (1), the counterions may be either condensed and immobilized on a chain or more loosely bound and free to move along a chain. These chain-localized (condensed or mobile) counterions tend to distribute uniformly along, and partially neutralize, the chains. In our model, counterions in regions (1) and (2) act to renormalize the bare macroion valence. The parameter Z thus should be physically interpreted as an *effective* macroion valence, generally much lower than the bare valence (number of ionizable monomers). From the Manning counterion condensation criterion [1], according to which the linear charge density of a PE chain saturates at $\sim e/\lambda_B$, we can expect the bare charge in an aqueous solution to be renormalized down by at least an order of magnitude.

The local number density profiles of charged monomers in the PE brushes, $\rho_{\text{mon}}(r)$, and of counterions, $\rho_c(r)$, are modeled here as continuous, spherically symmetric distributions. Charge discreteness can be reasonably neglected if we ignore structure on length scales shorter than the minimum separation between charges. Spherical symmetry of charge distributions can be assumed if intra-macroion chain-chain interactions, which favor isotropic distribution of chains, dominate over inter-macroion interactions, which favor anisotropy.

The density profile of charged monomers depends on the conformations of chains in the PE shells. Electrostatic repulsion between charged monomers tends to radially stretch and stiffen PE chains. Indeed, neutron scattering experiments [8] on diblock (neutral-charged) copolymer micelles, as well as simulations [24], provide strong evidence that the arms of spherical PE brushes can exhibit rodlike behavior. Here we assume the ideal case of fully stretched chains of equal length – a porcupine conformation [20] – and model the charged monomer number density profile by

$$\rho_{\text{mon}}(r) = \begin{cases} 0, & r > R \\ \frac{Z}{4\pi l r^2}, & a < r \leq R \\ 0, & r \leq a, \end{cases} \quad (1)$$

where r is the radial distance from the macroion's center. The model thus neglects configurational entropy of the PE chains, although it does include the entropy of the microions.

III. THEORY

For the model suspension defined above, our goal is to predict distributions of microions inside and outside of the PE brushes and effective interactions between macroions. Adapting the general response theory approach previously applied to charged colloids [26, 27, 28] and PE solutions [29], we reduce the multi-component mixture to an equivalent one-component system governed by effective interactions, and approximate the effective one-component Hamiltonian via perturbation theory. To simplify notation, we initially ignore salt ions. The Hamiltonian then decomposes, quite generally, into three terms:

$$H = H_m(\{\mathbf{R}\}) + H_c(\{\mathbf{r}\}) + H_{mc}(\{\mathbf{R}\}, \{\mathbf{r}\}), \quad (2)$$

where $\{\mathbf{R}\}$ and $\{\mathbf{r}\}$ denote collective coordinates of macroions and counterions, respectively. The first term in Eq. (2),

$$H_m = H_{\text{hc}} + \frac{1}{2} \sum_{i \neq j=1}^{N_m} v_{mm}(|\mathbf{R}_i - \mathbf{R}_j|), \quad (3)$$

is the macroion Hamiltonian, which includes a hard-core contribution H_{hc} (kinetic energy and hard-core interactions), and an electrostatic contribution due to the bare Coulomb pair interaction potential

$$v_{mm}(r) = \frac{Z^2 e^2}{\epsilon r} \quad (4)$$

at center-center separation r . The second term in Eq. (2),

$$H_c = K_c + \frac{1}{2} \sum_{i \neq j=1}^{N_c} v_{cc}(|\mathbf{r}_i - \mathbf{r}_j|), \quad (5)$$

is the Hamiltonian of the counterions with kinetic energy K_c interacting via the Coulomb pair potential $v_{cc}(r) = z^2 e^2 / \epsilon r$. The third term in Eq. (2),

$$H_{mc} = \sum_{i=1}^{N_m} \sum_{j=1}^{N_c} v_{mc}(|\mathbf{R}_i - \mathbf{r}_j|), \quad (6)$$

is the macroion-counterion interaction, which also may be expressed in the form

$$H_{mc} = \int d\mathbf{R} \rho_m(\mathbf{R}) \int d\mathbf{r} \rho_c(\mathbf{r}) v_{mc}(|\mathbf{R} - \mathbf{r}|), \quad (7)$$

where $\rho_m(\mathbf{R}) = \sum_{i=1}^{N_m} \delta(\mathbf{R} - \mathbf{R}_i)$ and $\rho_c(\mathbf{r}) = \sum_{j=1}^{N_c} \delta(\mathbf{r} - \mathbf{r}_j)$ are the macroion and counterion number density operators, respectively, and $v_{mc}(|\mathbf{R} - \mathbf{r}|)$ is the macroion-counterion interaction potential (to be specified in Sec. IV).

The mixture of macroions and counterions can be formally reduced to an equivalent one-component system by integrating out the counterion coordinates. Denoting traces over counterion and macroion coordinates by $\langle \rangle_c$ and $\langle \rangle_m$, respectively, the canonical partition function can be expressed as

$$\mathcal{Z} = \langle \langle \exp(-\beta H) \rangle_c \rangle_m = \langle \exp(-\beta H_{\text{eff}}) \rangle_m, \quad (8)$$

where $\beta = 1/k_B T$, $H_{\text{eff}} = H_m + F_c$ is the effective one-component Hamiltonian, and

$$F_c = -k_B T \ln \left\langle \exp \left[-\beta (H_c + H_{mc}) \right] \right\rangle_c \quad (9)$$

is the free energy of a nonuniform gas of counterions in the presence of the macroions.

Now regarding the macroions as an “external” potential for the counterions, we invoke perturbation theory [26, 27, 28, 30] and write

$$F_c = F_0 + \int_0^1 d\lambda \langle H_{mc} \rangle_\lambda, \quad (10)$$

where $F_0 = -k_B T \ln \langle \exp(-\beta H_c) \rangle_c$ is the reference free energy of the unperturbed counterions, the λ -integral charges the macroions (*i.e.*, the PE brushes) from neutral to fully charged, H_{mc} represents the perturbing potential of the macroions acting on the counterions, and $\langle H_{mc} \rangle_\lambda$ is the mean value of this potential in a suspension of macroions charged to a fraction λ of their full charge.

Two formal manipulations prove convenient. First, we convert the free energy of the unperturbed counterions to that of a classical one-component plasma (OCP) by adding and subtracting, on the right side of Eq. (10), the energy of a uniform compensating negative background [31], $E_b = -N_c n_c \hat{v}_{cc}(0)/2$. Here $n_c = N_c/[V(1 - \eta_{\text{hc}})]$ is the average density of counterions in the free volume – *i.e.*, the total volume reduced by the volume fraction $\eta_{\text{hc}} = (4\pi/3)n_m a^3$ of the macroion hard cores – and $\hat{v}_{cc}(0)$ is the $k \rightarrow 0$ limit of the Fourier transform of $v_{cc}(r)$. Equation (10) then becomes

$$F_c = F_{\text{OCP}} + \int_0^1 d\lambda \langle H_{mc} \rangle_\lambda - E_b, \quad (11)$$

where $F_{\text{OCP}} = F_0 + E_b$ is the free energy of a homogeneous OCP excluded from the colloidal hard cores. Second, we express H_{mc} in terms of Fourier components:

$$\langle H_{mc} \rangle_\lambda = \frac{1}{V} \sum_{\mathbf{k} \neq 0} \hat{v}_{mc}(k) \hat{\rho}_m(\mathbf{k}) \langle \hat{\rho}_c(-\mathbf{k}) \rangle_\lambda + \frac{1}{V} \lim_{k \rightarrow 0} [\hat{v}_{mc}(k) \hat{\rho}_m(\mathbf{k}) \langle \hat{\rho}_c(-\mathbf{k}) \rangle_\lambda], \quad (12)$$

where $\hat{v}_{mc}(k)$ is the Fourier transform of the macroion-counterion interaction and where $\hat{\rho}_m(\mathbf{k}) = \sum_{j=1}^{N_m} \exp(-i\mathbf{k} \cdot \mathbf{R}_j)$ and $\hat{\rho}_c(\mathbf{k}) = \sum_{j=1}^{N_c} \exp(-i\mathbf{k} \cdot \mathbf{r}_j)$ are Fourier components of the macroion and counterion number density operators. The $k = 0$ term is singled out because the number of counterions, $N_c = \hat{\rho}_c(0)$, does not respond to the macroion charge, but rather is fixed by the constraint of global charge neutrality.

Further progress requires approximations for the counterion free energy. Applying second-order perturbation (linear response) theory, the counterions are assumed to respond linearly to the macroion external potential:

$$\rho_c(\mathbf{r}) = \int d\mathbf{r}' \chi(\mathbf{r} - \mathbf{r}') \int d\mathbf{r}'' \rho_m(\mathbf{r}'') v_{mc}(\mathbf{r}' - \mathbf{r}'') \quad (13)$$

or

$$\hat{\rho}_c(\mathbf{k}) = \chi(k) \hat{v}_{mc}(k) \hat{\rho}_m(\mathbf{k}), \quad k \neq 0, \quad (14)$$

where $\chi(k)$ is the linear response function of the OCP.

Combining Eqs. (11)-(14), the effective Hamiltonian can be expressed in the form of the Hamiltonian of a one-component pairwise-interacting system:

$$H_{\text{eff}} = H_{\text{hc}} + \frac{1}{2} \sum_{i \neq j=1}^{N_m} v_{\text{eff}}(|\mathbf{R}_i - \mathbf{R}_j|) + E_0, \quad (15)$$

where $v_{\text{eff}}(r) = v_{mm}(r) + v_{\text{ind}}(r)$ is an effective electrostatic macroion-macroion pair interaction that augments the bare macroion interaction $v_{mm}(r)$ by a counterion-induced interaction

$$\hat{v}_{\text{ind}}(k) = \chi(k) [\hat{v}_{mc}(k)]^2. \quad (16)$$

The final term in Eq. (15) is the volume energy,

$$E_0 = F_{\text{OCP}} + \frac{N_m}{2} \lim_{r \rightarrow 0} v_{\text{ind}}(r) + N_m \lim_{k \rightarrow 0} \left[-\frac{1}{2} n_m \hat{v}_{\text{ind}}(k) + n_c \hat{v}_{mc}(k) + \frac{Z}{2z} n_c \hat{v}_{cc}(k) \right], \quad (17)$$

which emerges naturally from the one-component reduction. Although independent of the macroion coordinates, the volume energy depends on the average macroion density and

thus has the potential to significantly influence thermodynamics. Evidently, the effective interactions depend on the macroion structure through the specific form of the macroion-counterion interaction v_{mc} in Eqs. (16) and (17).

The OCP linear response function, proportional to the corresponding static structure factor $S(k)$, may be obtained from liquid-state theory [30]. In practice, the OCP is weakly correlated, with coupling parameter $\Gamma = \lambda_B/a_c \ll 1$, where $a_c = (3/4\pi n_c)^{1/3}$ is the counterion sphere radius. For example, for hard-sphere macroions of radius $a = 50$ nm, valence $Z = 500$, and volume fraction $\eta_{hc} = 0.01$, in water at room temperature ($\lambda_B = 0.714$ nm), we find $\Gamma \simeq 0.02$. As in previous work on charged colloids [27, 28] and polyelectrolytes [29], we adopt the random phase approximation (RPA), which is valid for weakly-coupled plasmas. The RPA equates the OCP two-particle direct correlation function to its exact asymptotic limit: $c^{(2)}(r) = -\beta v_{cc}(r)$. Using the Ornstein-Zernike relation, $S(k) = 1/[1 - n_c \hat{c}^{(2)}(k)]$, the linear response function then takes the form

$$\chi(k) = -\beta n_c S(k) = -\frac{\beta n_c}{(1 + \kappa^2/k^2)}, \quad (18)$$

where $\kappa = \sqrt{4\pi n_c z^2 \lambda_B}$ is the Debye screening constant (inverse screening length). Note that the screening constant, which involves the density of counterions in the free volume, naturally incorporates the excluded volume of the macroion cores. With $\chi(k)$ specified, the counterion density can be calculated from the macroion-counterion interaction and Eq. (14) for a given macroion distribution (see Sec. IV). Finally, salt ions can be easily incorporated by introducing additional response functions [28]. The pair interaction and volume energy are then modified only through a redefinition of the Debye screening constant: $\kappa = \sqrt{4\pi(n_c + 2n_s)z^2 \lambda_B}$, where $n_s = N_s/[V(1 - \eta_{hc})]$ is the average number density of salt ion pairs in the free volume.

Generalization of response theory to incorporate leading-order nonlinear microion response entails three-body effective interactions, as well as corrections to the effective pair potential and volume energy [32]. Nonlinear effects are generally significant, however, only in concentrated, deionized suspensions of highly charged macroions [32] and are here ignored. It has been shown that response theory, combined with the RPA, is formally equivalent to Poisson-Boltzmann theory [32]. Both approaches rely on mean-field approximations that neglect microion fluctuations and predict microion distributions of the same general form, aside from a distinction in the screening constant, which response theory corrects for excluded vol-

ume of the macroion cores. Advantages of response theory over Poisson-Boltzmann theory are its predictions of (1) the entire effective Hamiltonian, including the one-body volume energy, which is essential for a complete description of phase behavior [26, 27, 28, 33, 34, 35, 36], and (2) a more accurate expression for the Debye screening constant that incorporates the macroion excluded-volume correction.

IV. ANALYTICAL RESULTS

For our porcupine model of a spherical PE brush with $1/r^2$ monomer density profile, Gauss's law gives the electric field around a macroion as

$$E(r) = \begin{cases} -\frac{Ze}{\epsilon} \frac{1}{r^2}, & r > R \\ -\frac{Ze}{\epsilon} \frac{r-a}{lr^2}, & a < r \leq R \\ 0, & r \leq a. \end{cases} \quad (19)$$

Integration over r yields the electrostatic potential energy between a brush and a counterion:

$$v_{mc}(r) = \begin{cases} -\frac{Zze^2}{\epsilon r}, & r > R \\ -\frac{Zze^2}{\epsilon l} \left[1 - \frac{a}{r} - \ln\left(\frac{r}{R}\right) \right], & a < r \leq R \\ -\frac{Zze^2}{\epsilon l} \left[\alpha - \ln\left(\frac{a}{R}\right) \right], & r \leq a, \end{cases} \quad (20)$$

where α is an arbitrary constant, which arises because $v_{mc}(r)$ is not uniquely defined inside the hard core. Following van Roij and Hansen [35], we choose α below by requiring that the counterion density vanish inside the hard core. Fourier transforming Eq. (20) yields

$$\hat{v}_{mc}(k) = -\frac{4\pi Zze^2}{\epsilon k^3 l} G(ka, kR; \alpha), \quad (21)$$

where the function $G(ka, kR; \alpha)$ is defined as

$$G(x_1, x_2; \alpha) = \text{sinc}(x_2) - \text{sinc}(x_1) - \alpha[x_1 \cos(x_1) - \sin(x_1)], \quad (22)$$

with $\text{sinc}(x) \equiv \int_0^x du \sin(u)/u$. We can now calculate, in the dilute limit, the counterion number density profile around a single macroion, taking $\hat{\rho}_m(\mathbf{k}) = 1$. From Eqs. (14), (18), and (21), the Fourier component of the density profile is

$$\hat{\rho}_c(k) = \frac{Z}{z} \frac{\kappa^2}{kl(k^2 + \kappa^2)} G(ka, kR; \alpha), \quad (23)$$

which in real space takes the form

$$\rho_c(r) = \frac{Z}{z} \frac{\kappa}{4\pi l r} \begin{cases} S(\kappa a, \kappa R; \alpha) e^{-\kappa r}, & r > R \\ S(\kappa a, \kappa r; \alpha) e^{-\kappa r} + \text{Ec}(-\kappa r, -\kappa R) \sinh(\kappa r), & a < r \leq R \\ [\text{Ec}(-\kappa a, -\kappa R) + \alpha(1 + \kappa a) e^{-\kappa a}] \sinh(\kappa r), & r \leq a. \end{cases} \quad (24)$$

For simplicity, we have introduced two functions, $S(x_1, x_2; \alpha)$ and $\text{Ec}(x_1, x_2)$, which are defined, respectively, as

$$S(x_1, x_2; \alpha) = \text{shi}(x_2) - \text{shi}(x_1) - \alpha[x_1 \cosh(x_1) - \sinh(x_1)] \quad (25)$$

and

$$\text{Ec}(x_1, x_2) = \text{Ei}(x_2) - \text{Ei}(x_1), \quad (26)$$

where $\text{shi}(x) \equiv \int_0^x du \sinh(u)/u$ denotes the hyperbolic sine integral function and $\text{Ei}(x) \equiv \int_{-\infty}^x du e^u/u$ is the exponential integral function. Now setting the counterion density to zero within the hard core [*i.e.*, $\rho_c(r) = 0, r \leq a$, in Eq. (24)] fixes the constant α :

$$\alpha = -\frac{e^{\kappa a}}{1 + \kappa a} \text{Ec}(-\kappa a, -\kappa R). \quad (27)$$

Integrating Eq. (24) over the spherical shell volume of a PE brush yields the fraction of counterions inside a brush:

$$f_{\text{in}} = 1 - \frac{1 + \kappa R}{\kappa l} e^{-\kappa R} S(\kappa a, \kappa R; \alpha). \quad (28)$$

From this expression, it is clear that the counterion distribution, within the model, is determined entirely by two independent dimensionless parameters, κa and κl , *i.e.*, the ratios of the macroion core radius and brush thickness, respectively, to the Debye screening length.

From Eqs. (16) and (21), the induced electrostatic pair interaction is given by

$$\hat{v}_{\text{ind}}(k) = -\frac{4\pi Z^2 e^2}{\epsilon} \frac{\kappa^2}{l^2 k^4 (k^2 + \kappa^2)} [G(\kappa a, \kappa R; \alpha)]^2, \quad (29)$$

whose Fourier transform is

$$v_{\text{ind}}(r) = -\frac{2Z^2 e^2 \kappa^2}{\pi \epsilon l^2 r} \int_0^\infty dk \frac{\sin(kr)}{k^3 (k^2 + \kappa^2)} [G(\kappa a, \kappa R; \alpha)]^2. \quad (30)$$

For nonoverlapping brushes, Eq. (30) can be reduced to the analytical form

$$v_{\text{ind}}(r) = -\frac{Z^2 e^2}{\epsilon r} + \frac{Z^2 e^2}{\epsilon} \left[\frac{S(\kappa a, \kappa R; \alpha)}{\kappa l} \right]^2 \frac{e^{-\kappa r}}{r}, \quad r > 2R. \quad (31)$$

After adding to Eq. (31) the bare Coulomb potential between the spherical macroions [Eq. (4)], the residual effective pair interaction is

$$v_{\text{eff}}(r) = \frac{Z^2 e^2}{\epsilon} \left[\frac{S(\kappa a, \kappa R; \alpha)}{\kappa l} \right]^2 \frac{e^{-\kappa r}}{r}, \quad r > 2R. \quad (32)$$

Thus, within the coarse-grained PE brush model and at the level of linear response theory, nonoverlapping PE brushes are predicted to interact via an effective Yukawa pair potential of the same screened-Coulomb form as the long-range limit of the DLVO potential [37] for charged colloids. This result is consistent with previous linear response results for charged hard spheres [27, 28], which interact via the DLVO effective pair potential

$$v_{\text{eff}}(r) = \frac{Z^2 e^2}{\epsilon} \left(\frac{e^{\kappa R}}{1 + \kappa R} \right)^2 \frac{e^{-\kappa r}}{r}, \quad r > 2R, \quad (33)$$

and for PE stars [29], which interact via

$$v_{\text{eff}}(r) = \frac{Z^2 e^2}{\epsilon} \left[\frac{\text{shi}(\kappa R)}{\kappa R} \right]^2 \frac{e^{-\kappa r}}{r}, \quad r > 2R. \quad (34)$$

Note that the screening constant, κ , in the pair potential depends on the total density of microions – inside and outside of the brushes – since all microions respond to the macroion charge. We do not consider here overlapping brushes, in which case steric interactions between chains also should be included [24].

Finally, the volume energy is obtained from Eqs. (17), (21), (29), and (30), as

$$E_0 = F_{\text{OCP}} - N_m \frac{Z^2 e^2 \kappa^2}{\pi \epsilon l^2} \int_0^\infty dk \frac{[G(ka, kR; \alpha)]^2}{k^2(k^2 + \kappa^2)} - (N_+ - N_-) \frac{k_B T}{2}. \quad (35)$$

Assuming weakly-coupled microion plasmas, the OCP free energy is well approximated by its ideal-gas limit:

$$F_{\text{OCP}} = N_+ [\ln(n_+ \Lambda_+^3) - 1] + N_- [\ln(n_- \Lambda_-^3) - 1], \quad (36)$$

where Λ_\pm are the thermal de Broglie wavelengths of the positive/negative microions. The physical interpretation of the volume energy is straightforward. The first term on the right side of Eq. (35) represents the entropy of free microions, the second term the electrostatic energy of microion-macroion interactions, and the third term accounts for the background subtraction. If the macroion valence Z is allowed to vary with concentration (*e.g.*, through

counterion condensation), then E_0 should be supplemented by the macroion self energy. We emphasize that, because of its dependence on the average macroion concentration, the volume energy has the potential to influence thermodynamic phase behavior. As a check of the present results, it can be shown that in the two limiting cases of vanishing PE shell thickness ($l \rightarrow 0$, with Z fixed) and, independently, vanishing hard core diameter ($a \rightarrow 0$) all analytical results reduce to those given in refs. [27, 28] and [29], respectively.

V. NUMERICAL RESULTS AND DISCUSSION

To illustrate applications of the theory developed above, we present numerical results for the case of monovalent counterions ($z = 1$) in aqueous suspensions at room temperature ($\lambda_B = 0.714$ nm). Figure 2 shows the predicted counterion profiles around three different types of macroion, all of the same outer radius $R = 50$ nm, valence $Z = 500$, and reduced number density $n_m R^3 = 0.01$, for a salt-free suspension. The chosen valence is within the upper limit suggested by charge renormalization theory [38] for this size of macroion: $Z < \mathcal{O}(10)R/\lambda_B$. For a star macroion, the counterion density diverges logarithmically towards the center [29], while for brush-coated and bare hard-sphere macroions the counterion densities remain finite. Figure 3 displays the corresponding internal counterion fraction, *i.e.*, fractional counterion penetration, as a function of κR . For fixed ratio of hard-core radius to outer radius, a/R , the internal counterion fraction increases monotonically with κR , reflecting increasing permeability of the macroions to counterions with decreasing screening length (*e.g.*, increasing salt concentration). On the other hand, when κR is fixed, the counterion penetration decreases upon thinning of the PE brush (increasing a/R). In the limit of vanishing brush thickness ($l/R \rightarrow 0$, $a/R \rightarrow 1$), Eq. (28) reduces to

$$f_{\text{in}}(l \rightarrow 0) = \frac{\kappa a}{\kappa a + 1} \kappa l + O(l^2). \quad (37)$$

Counterions are predicted to penetrate PE brush-coated macroions less efficiently than stars.

Penetration of macroions by counterions can strongly influence screening of bare Coulomb interactions. Thus, effective pair interactions between brush-coated macroions depend sensitively on the thickness of the PE brush. To illustrate, Fig. 4 shows the effective pair potential for the same three macroion types as in Figs. 2 and 3 and for two salt concentrations, $c_s = 0$

M and $c_s = 100 \mu\text{M}$, corresponding to different Debye screening constants κ . For identical system parameters, the strength of the Yukawa pair interaction for nonoverlapping brush macroions is intermediate between that for hard-sphere and star macroions. Figure 5 compares the dependence of the macroion-size-dependent amplitude of $v_{\text{eff}}(r)$, $r > 2R$, on Debye screening constant for the three macroion types. The amplitude increases with κR for fixed ratio of hard-core to outer radius, while for fixed κR the amplitude increases from the star limit to the hard-sphere limit as the PE brush thins to infinitesimal thickness ($a/R \rightarrow 1$).

VI. CONCLUSIONS

Summarizing, polyelectrolyte-coated colloids provide a valuable conceptual bridge between charged colloids and polyelectrolytes. In this paper, linear response theory is applied to bulk suspensions of spherical colloidal particles coated with PE brushes. Assuming stiff, radially stretched PE chains, we model each brush as a spherically symmetric shell of continuously distributed charge, the charge density varying with radial distance r as $1/r^2$. By formally integrating out the microion degrees of freedom, the Hamiltonian of the macroion-microion mixture is mapped onto the effective Hamiltonian of an equivalent one-component system. Predictions of the theory include microion density profiles, effective electrostatic interactions between pairs of (nonoverlapping) macroions, and a state-dependent one-body volume energy, which contributes to the total free energy. The theory presented here may provide a practical guide for choosing system parameters to achieve desired interactions.

The main conclusions of this study are: (1) Trapping of counterions inside a spherical PE brush is highly sensitive to variations in the core radius, brush thickness, and Debye screening length of the solution. For fixed ratio of core to outer radius, the fraction of trapped counterions increases monotonically with increasing outer radius or decreasing screening length. For fixed ratio of outer radius to screening length, the fraction of trapped counterions decreases monotonically from a maximum in the limit of vanishing core radius (PE star macroion) to zero in the limit of vanishing shell thickness (hard-sphere macroion). (2) Within the linear response approximation, the effective pair interaction between nonoverlapping macroions has a Yukawa (screened-Coulomb) form. (3) By varying core radius and brush thickness, effective interactions between PE brush-coated macroions can be tuned – in both amplitude

and range – between interactions for hard-sphere and star macroions. For fixed ratio of core radius to outer radius, the amplitude of the pair interaction increases monotonically with increasing outer radius or decreasing screening length, while for fixed ratio of outer radius to screening length, the amplitude increases monotonically from the star-limit to the hard-sphere limit. The range of the pair interaction, governed by the Debye screening length, depends on the hard-core volume fraction and so can be varied by adjusting the core radius.

The range of validity of the coarse-grained model and linearized theory studied here, and the accuracy of the predicted Yukawa form of effective pair interaction, including amplitude and range, could be directly tested by future simulations of more explicit models of PE-grafted colloids. Our purely electrostatic model can be augmented by chain elasticity and entropy – essential for describing overlapping PE shells [24]. The mean-field linear response theory can be refined to incorporate nonlinear microion response [32] and microion correlations, beyond the random phase approximation. The theory also can be easily adapted to other macroion types, such as core-shell microgels [29, 39]. Future work will explore thermodynamic phase behavior, which we anticipate to be quite rich and tunable between that of charge-stabilized colloidal suspensions and polyelectrolyte solutions.

Acknowledgments

This work was supported by the National Science Foundation under Grant Nos. DMR-0204020 and EPS-0132289.

-
- [1] F. Oosawa, *Polyelectrolytes* (Dekker, New York, 1971).
 - [2] *Polyelectrolytes*, ed. M. Hara (Dekker, New York, 1993).
 - [3] R. Tuinier and C. G. de Kruif, *J. Chem. Phys.* **117**, 1290 (2002).
 - [4] D. F. Evans and H. Wennerström, *The Colloidal Domain*, 2nd ed. (Wiley-VCH, New York, 1999).
 - [5] R. J. Hunter, *Foundations of Colloid Science* (Oxford, New York, 1986).
 - [6] X. Guo and M. Ballauff, *Phys. Rev. E* **64**, 051406 (2001).

- [7] Y. Mir, P. Auroy, and L. Auvray, *Phys. Rev. Lett.* **75**, 2863 (1995).
- [8] P. Guenoun, F. Muller, M. Delsanti, L. Auvray, Y. J. Chen, J. W. Mays, and M. Tirrell, *Phys. Rev. Lett.* **81**, 3872 (1998).
- [9] W. Groenewegen, S. U. Egelhaaf, A. Lapp, and J. R. C. van der Maarel, *Macromol.* **33**, 3283 (2000).
- [10] Y. Tran, P. Auroy, L.-T. Lee, and M. Stamm, *Phys. Rev. E* **60**, 6984 (1999).
- [11] R. Hariharan, C. Biver, J. Mays, and W. B. Russel, *Macromol.* **31**, 7506 (1998).
- [12] Y. Mei, A. Wittemann, G. Sharma, M. Ballauff, Th. Koch, H. Gliemann, J. Horbach, and Th. Schimmel, *Macromol.* **36**, 3452 (2003).
- [13] S. J. Miklavic and S. Marčelja, *J. Phys. Chem.* **92**, 6718 (1988).
- [14] S. Misra, S. Varanasi, and P. P. Varanasi, *Macromol.* **22**, 4173 (1989).
- [15] S. Misra, M. Tirrell, and W. Mattice, *Macromol.* **29**, 6056 (1996).
- [16] E. B. Zhulina and O. V. Borisov, *J. Chem. Phys.* **107**, 5952 (1997).
- [17] E. Gurovitch and P. Sens, *Phys. Rev. Lett.* **82**, 339 (1999).
- [18] O. V. Borisov, F. A. M. Leermakers, G. J. Fleer, and E. B. Zhulina, *J. Chem. Phys.* **114**, 7700 (2001).
- [19] J. Klein Wolterink, J. van Male, M. Daoud, and O. V. Borisov, *Macromol.* **36**, 6624 (2003).
- [20] P. Pincus, *Macromol.* **24**, 2912 (1991).
- [21] H. Schiessel and P. Pincus, *Macromol.* **31**, 7953 (1998).
- [22] S. J. Miklavic, C. E. Woodward, Bo Jönsson, and T. Åkesson, *Macromol.* **23**, 4149 (1990).
- [23] F. S. Csajka and C. Seidel, *Macromol.* **33**, 2728 (2000).
- [24] A. Jusufi, C. N. Likos, and H. Löwen, *Phys. Rev. Lett.* **88**, 018301 (2002); *J. Chem. Phys.* **116**, 11011 (2002).
- [25] R. Podgornik, T. Åkesson, and Bo Jönsson, *J. Chem. Phys.* **102**, 9423 (1995).
- [26] M. J. Grimson and M. Silbert, *Mol. Phys.* **74**, 397 (1991); E. Canessa, M. J. Grimson, and M. Silbert, *Mol. Phys.* **64**, 1195 (1988); in *Strongly Coupled Plasma Physics*, ed. S. Ichimaru (Elsevier/Yamada Science Foundation, 1990), p. 675.
- [27] A. R. Denton, *J. Phys.: Condens. Matter* **11**, 10061 (1999).
- [28] A. R. Denton, *Phys. Rev. E* **62**, 3855 (2000).

- [29] A. R. Denton, *Phys. Rev. E* **67**, 011804 (2003).
- [30] J.-P. Hansen and I. R. McDonald, *Theory of Simple Liquids*, 2nd ed. (Academic, London, 1986).
- [31] The background energy, which is infinite for point counterions, formally cancels corresponding infinities in the counterion and macroion-counterion Hamiltonians [Eqs. (5) and (6)].
- [32] A. R. Denton, *Phys. Rev. E* (in press).
- [33] R. van Roij and J.-P. Hansen, *Phys. Rev. Lett.* **79**, 3082 (1997).
- [34] H. Graf and H. Löwen, *Phys. Rev. E* **57**, 5744 (1998).
- [35] R. van Roij, M. Dijkstra, and J. P. Hansen, *Phys. Rev. E* **59**, 2010 (1999).
- [36] P. B. Warren, *J. Chem. Phys.* **112**, 4683 (2000).
- [37] E. J. W. Verwey and J. T. G. Overbeek, *Theory of the Stability of Lyophobic Colloids* (Elsevier, Amsterdam, 1948).
- [38] S. Alexander, P. M. Chaikin, P. Grant, G. J. Morales, and P. Pincus, *J. Chem. Phys.* **80**, 5776 (1984).
- [39] T. Hellweg, C. D. Dewhurst, W. Eimer, and K. Kratz, *Langmuir* **20**, 4330 (2004).

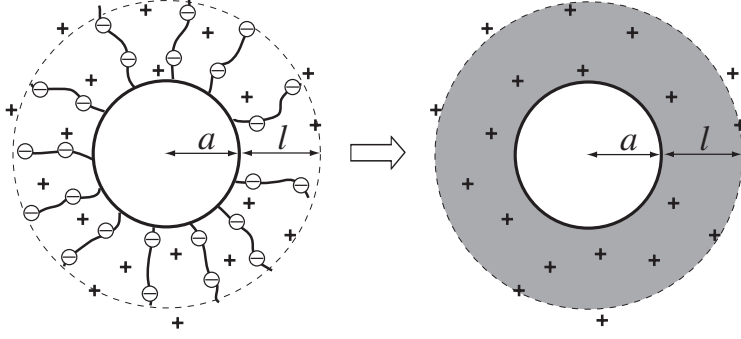


FIG. 1: (a) Polyelectrolyte (PE) brush-coated colloidal sphere and, (b) model considered here, in which the PE monomer charge distribution is assumed continuous and varying as $1/r^2$, $a < r < a+l$.

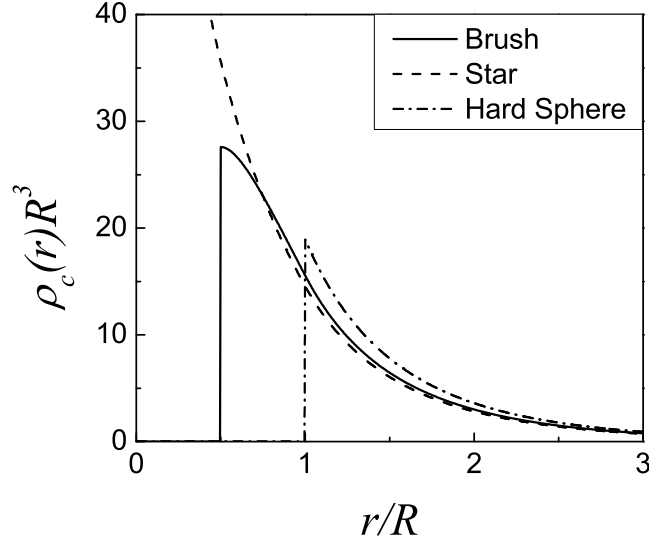


FIG. 2: Counterion number density profiles of three types of spherical macroion of outer radius $R = 50$ nm, valence $Z = 500$, and reduced number density $n_m R^3 = 0.01$ in water at room temperature ($\lambda_B = 0.714$ nm): PE brush-coated macroion [solid curve from Eq. (24)], PE star [dashed curve from Eq. (20) of ref. [29]], and charged hard sphere [dot-dashed curve from Eq. (32) of ref. [27]]. For the brush-coated macroion, the hard-core radius is $a = 25$ nm and the PE shell thickness is $l = 25$ nm.

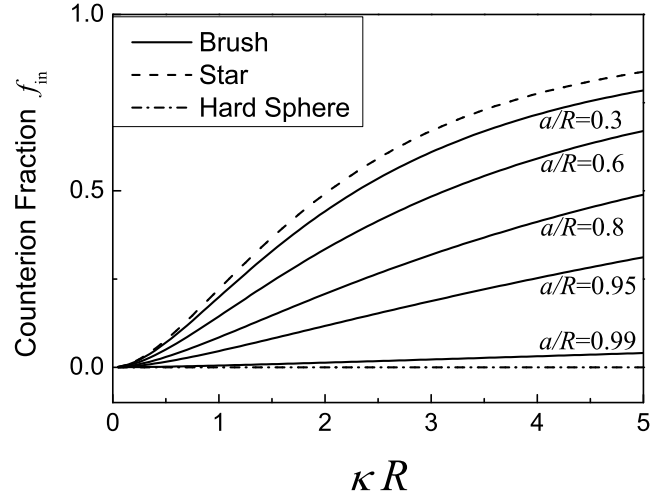


FIG. 3: Fraction of counterions [from Eq. (28)] trapped inside PE brush as a function of the dimensionless parameter κR (ratio of outer radius to Debye screening length) for several values of a/R (ratio of core radius to outer radius).

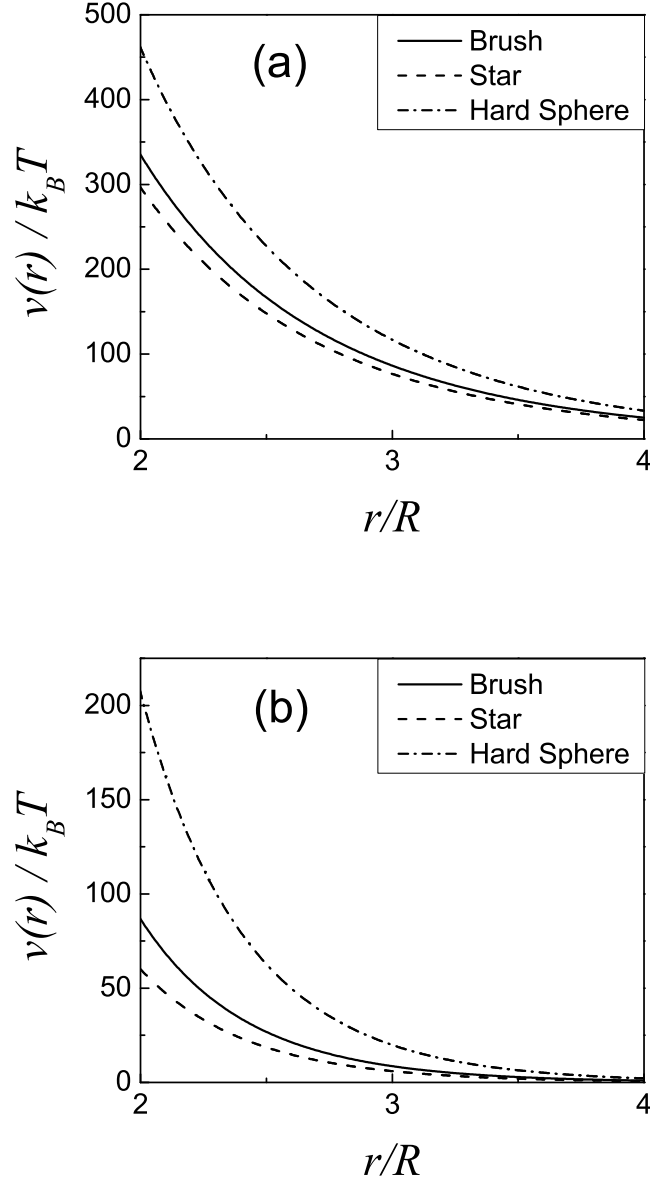


FIG. 4: Effective electrostatic interactions between pairs of nonoverlapping macroions of outer radius $R = 50$ nm, valence $Z = 500$, and reduced number density $n_m R^3 = 0.01$ in room temperature water ($\lambda_B = 0.714$ nm) at salt concentrations (a) $c_s = 0$ mol/l ($\kappa R \simeq 0.95$) and (b) $c_s = 100$ μ mol/l ($\kappa R \simeq 1.9$): PE brush-coated spherical macroions [solid curves from Eq. (32)]; PE stars [dashed curves from Eq. (34)]; and charged hard spheres [dot-dashed curves from Eq. (33)].

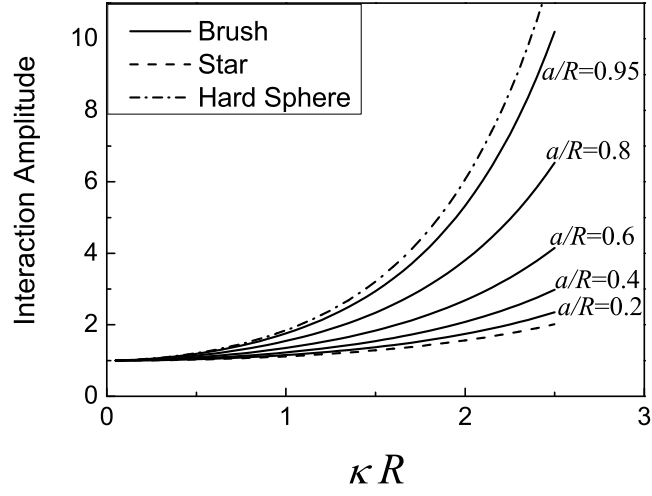


FIG. 5: Amplitude of Yukawa effective electrostatic interactions between pairs of nonoverlapping brushes, stars and charged hard spheres vs. Debye screening constant, normalized to unity at $\kappa R = 0$ [from Eqs. (32)-(34)].